Chemical Engineering Science 146 (2016) 291–301

Contents lists available at ScienceDirect

Chemical Engineering Science

journal homepage: www.elsevier.com/locate/ces

Competitive adsorption of surfactant–protein mixtures in a continuous stripping mode foam fractionation column

Ishara Dedunu Kamalanathan, Peter James Martin *

School of Chemical Engineering and Analytical Science, The University of Manchester, Manchester M13 9PL, UK

HIGHLIGHTS

- Competitive adsorption shown in a binary stripping mode foam fractionation column.
- Analytical characterisation of protein (BSA) and surfactant (Triton X–100) system.
- Foam stabilised by BSA with negligible Triton X–100 in bottom product.
- Triton X–100 has higher surface activity than BSA and displaced it from interface.

GRAPHICAL ABSTRACT

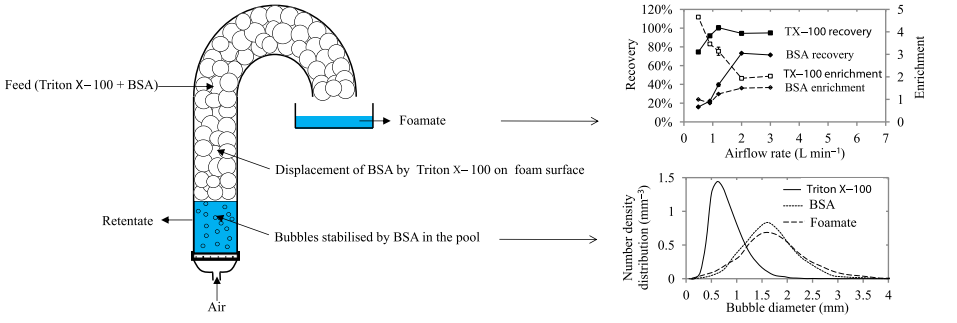

ARTICLE INFO

Article history:
Received 8 January 2016
Received in revised form
17 February 2016
Accepted 1 March 2016
Available online 9 March 2016

Keywords:
Competitive adsorption
Surface activity
Foam fractionation
Bioseparation
Downstream processing
Surfactant

ABSTRACT

In this paper a detailed experimental study on the application of continuous stripping mode foam fractionation to separate a model surfactant–protein mixture was performed with emphasis on the competitive adsorption behaviour and transport processes of surfactant–protein mixtures in the rising foam column. Bubble size measurements of the foamate showed that at steady state conditions the bubbles rising from the liquid pool were stabilised by BSA. However at the top of the column the recovery of Triton X – 100 in the foamate (75–100%) was always greater than the recovery of BSA (13–76%) for all foam fractionation experiments. The enrichment of BSA remained at almost unity for experiments with high feed concentrations of both components and low air flow rates, and only increased when the recovery of Triton X – 100 reached 100%. Thus it was concluded that Triton X–100 displaced the adsorbed BSA from the surface. The surface activity and diffusivity of the two components was determined from surface tension and nuclear magnetic resonance (NMR) measurements. These results illustrated that competitive adsorption behaviour was due to the greater maximum surface pressure (2.05 times) and diffusivity (19.6 times) of Triton X – 100 than BSA. In addition to investigating the effect of foam fractionation process parameters on the separation of mixed systems, the results from the characterisation studies of surface adsorption and foam properties provided insight and deeper understanding of the competitive adsorption behaviour of surfactants and proteins in a foam fractionation process.

1. Introduction

Mixed surfactant protein systems are an important class of chemical in industrial products and processes. In the food industry surfactant–protein mixtures such as fatty acids and whey proteins are widely used for the stabilisation of foams and emulsions

* Corresponding author. Tel.: +44 161 306 4388.
E-mail address: p.martin@manchester.ac.uk (P.J. Martin).

http://dx.doi.org/10.1016/j.ces.2016.03.002

(Miller et al., 2005). Surfactant–protein mixtures are particularly significant in bioproducts such as biosurfactants and biopolymers where fermented products tend to be dilute mixtures of surface active components such as surfactant and protein (Winterburn and Martin, 2012). This complicates the downstream process and makes a universalised approach difficult. Currently a major barrier to commercialisation of bioproducts is expensive and inefficient downstream processing, for example Burghoff (2012) estimates these as 80 per cent of production costs. Thus there is a need to understand the separation science of such mixtures to improve the efficiency and effectiveness of downstream processing of such systems.

Foam fractionation has drawn most attention due to its low cost, mild conditions, sustainable approach where solvents are not required, the ability to process dilute solutions with high separation efficiency and the possibility for batchwise or continuous operation (Stevenson, 2012). It is a foam based separation process based on the preferential adsorption of surface active molecules on to an air-water surface (Lemlich, 1968). In a foam fractionation process, foam is created and stabilised at the bottom of a vertical column. Depending on factors such as pool volume, residence time of bubbles in pool and air flow rate, the foam may or may not be in equilibrium. The foam generated in a foam fractionation process consists of gas bubbles surrounded by liquid film lamellae. The lamellae intersect to form a network of Plateau borders and these connect at vertices. As the foam rises up the column, downwards drainage of interstitial liquid occurs in the Plateau border and vertices due to gravity and capillary forces. The contribution of capillary drainage typically becomes negligible by a foam height of around 50 mm such that the rising foam approaches a constant liquid hold up with column height (Martin et al., 2010). This foam product often called the foamate is enriched in surfactant and is collapsed to form a surfactant rich solution (Lemlich, 1972).

Foam fractionation can be operated in batch or continuous modes. The simplest mode of operation is the batch mode where an aqueous surfactant solution is sparged with gas until the surfactant concentration in the pool falls below the foaming concentration. However for steady state conditions to be achieved the process has to be run in continuous mode. There are two modes of continuous operation; simple and stripping mode. In a simple continuous process, feed is continuously fed into the bottom liquid pool whilst foam and a fraction of the bottom liquid pool are removed from the top and bottom of the column respectively. In a continuous stripping mode foam fractionation process, feed is injected near the top of column into the rising foam. Below the feed point a relatively wet rising foam is created; above the feed point the liquid in the foam drains and the foam becomes drier.

Bubbles are stabilised in the bottom pool and rise as a foam up the column. The feed will predominantly drain downwards through the centres of the Plateau border channels of the foam with some mixing at the vertices. Surfactant in the feed has the opportunity to diffuse from the centre of the Plateau border channels to their subsurface, and then adsorb to the interface. From the Plateau border-air interface, surfactant transport onto and throughout the lamellae films can occur through diffusive and Marangoni surface effect, which are coupled with the film drainage. The relative diffusive, adsorptive and interface properties of the different surfactant species can result in varying ratios of surface excess and therefore different separation effects. The transport and flow of surfactant through Plateau borders and on to foam lamellae have been described in previous theoretical studies (Vitasari et al., 2013b; Grassia et al., 2016; Vitasari et al., 2016).

The adsorptive separation of multicomponent systems in a foam fractionation process has been widely reported in the literature. The reported multicomponent systems include protein mixtures commonly found in milk and egg (Brown et al., 1999; Lockwood et al., 2000; Saleh and Hossain, 2001; Linke and Berger, 2011), surfactant mixtures, surfactant/metal ion mixtures and metal ion mixtures found in waste water (Qu et al., 2008; Rujirawanich et al., 2012; Micheau et al., 2015). Surfactants such as cetyl trimethyl ammonium bromide (CTAB) have been used to boost and assist the recovery of algae, enzymes, proteins, textile dyes and metal ions (Walkowiak and Grieves, 1976; Lockwood et al., 1997; Gerken et al., 2006; Lu et al., 2010; Xu et al., 2010; Coward et al., 2014). Components such as enzymes and proteins generally have lower surface activity compared to surfactants. For example Xu et al. (2010) investigated the use of nonionic surfactant Tween 20 to boost the foaming of a mixture of Bovine serum albumin (BSA) with antifoam agent polyoxypropylene polyoxyethylene glylerin ether (PGE). BSA reduces the surface tension of water from 73 mN m^{-1} to 53 mN m^{-1} (Makievski et al., 1998) whilst Tween 20 reduces the surface tension of water to 35 mN m^{-1} (Niño and Patino, 1998). Therefore Tween 20 was used to increase the foam generation and stability of BSA in the foam fractionation process. More recently Liu et al. (2015) reported on the use of biosurfactant rhamnolipid as a foam stabiliser to assist in the foam fractionation separation of carotenoid lycopene from tomato-based processing wastewater.

Most of the aforementioned foam fractionation studies were performed in batch mode. The exceptions are Brown et al. (1999), performed in continuous simple mode, Gerken et al. (2006) and Qu et al. (2008), performed in continuous stripping mode and Rujirawanich et al. (2012), performed in a continuous multistage foam fractionation system. Brown et al. (1999), Gerken et al. (2006), Qu et al. (2008) and Rujirawanich et al. (2012) investigated the effect of process and design parameters such as air flow rate, feed flow rate, feed concentration and column height on the separation of multicomponent systems. These studies reported that the component with the highest surface activity was found to have greatest recovery and enrichment. These results are indicative of competitive adsorption processes, but this aspect was not explored in any further detail.

Studies considering the competitive adsorption of multicomponent systems in a foam fractionation process are relatively uncommon. Rujirawanich et al. (2012) applied the concept of competitive adsorption to its study of the separation of surfactant mixtures of cationic cetylpyridinium chloride (CPC) and nonionic Triton X−100 using a continuous multistage foam fractionation system. However the complexity of the multistage system limited the depth of insight into the fundamentals of the process. Conclusions generally empirically correlated the separation efficiency to operating parameters.

A previous theoretical study (Vitasari et al., 2013a) investigated the competitive adsorption of mixed surfactant–protein systems at an air-water surface. The simulation results illustrated how the competitive adsorption between the nonionic surfactant decyl dimethyl phosphine oxide (C_{10}DMPO) and protein Bovine beta lactoglobulin (β-LG) depended on the relative diffusivity and surface affinity of the two components. Initially the surfactant with the higher diffusivity and lower surface affinity was found to arrive at air bubble surface. The surfactant was then displaced from the surface once the protein arrived at a later time. The study concluded that surfactants with high diffusivity and low surface affinity relative to proteins were more likely to be displaced by high surface affinity proteins.

The objective of this paper is to perform a detailed experimental study on the application of foam fractionation to separate a model surfactant–protein mixture and elucidate the competitive adsorption process. The foam fractionation experiments were performed with an emphasis of gaining a deeper understanding of the competitive adsorption behaviour and transport processes of surfactant–protein mixtures in a foam fractionation column. The

mixed surfactant–protein system selected was Triton X−100/ BSA mixture where the surface properties of Triton X−100 and BSA are both well characterised and for ease of concentration measurement. It was hypothesised that competitive adsorption between the surfactant species would play a significant role when the two species were at feed concentrations close to those that would just saturate the available foam surface area. Thus feed concentrations of surfactant and protein for the foam fractionation experiments were selected to be close to their CMCs. Experimental foam fractionation studies of surfactant–protein mixtures were supported with foam bubble size measurements, surface tension and NMR measurements to gain insight and deeper understanding of the competitive adsorption behaviour.

2. Materials and methods

2.1. Model choice of surfactant–protein mixture for foam fractionation studies

Due to the complex nature of ionic surfactant and protein interaction, only nonionic surfactant and protein systems are dealt with in this study. Ionic surfactants and proteins form surfactant–protein complexes via electrostatic interactions whilst mixed adsorption for nonionic surfactants and protein is mainly determined by competitive adsorption between the two components (Miller et al., 2000; Mackie, 2004).

Triton X−100 and BSA were selected because of their high surface activity, foaming ability and stability, adsorption properties and ease of concentration measurement. Although both components had UV absorbing groups, they both absorbed at similar wavelength ranges. Thus high performance liquid chromatography (HPLC) with an UV detector was used to detect and determine the concentrations of the two components. The HPLC method developed is described in Section 2.3.5.

2.2. Materials and sample preparation

Nonionic surfactant Triton X−100 (0.647 kDa) was obtained from Sigma-Aldrich, United Kingdom. Bovine serum albumin (BSA, A1470, a 66 kDa globular protein) was obtained from Sigma-Aldrich, United Kingdom. Triton X−100 and BSA were used with further purification.

For the surface tension measurements, solutions of the nonionic surfactant Triton X−100 were prepared with bi distilled water. Solutions of BSA were made using a phosphate buffer solution of strength 0.01 M at pH 7. The phosphate buffer solutions were prepared by appropriate stock solutions of Na_2HPO_4 and NaH_2PO_4. For the NMR measurements, Triton X−100 and BSA solutions were prepared with deuterium oxide 99.9 atom% (D_2O). For the foam fractionation and foam bubble size experiments, solutions of Triton X−100 and BSA were prepared with bi distilled water. Triton X−100 and BSA mixtures were made by mixing equal volumes of both components. All samples analysed by HPLC were filtered with a 0.2 μm filter membrane.

2.3. Methods

2.3.1. Surface tension

A Kruss tensiometer with a roughened Wilhelmy platinum plate of dimensions 19.9 mm × 10 mm × 0.2 mm (width, height and thickness respectively) was used to measure equilibrium surface tensions of Triton X−100 and BSA. The plate was cleaned via a flame until it turned red hot and then allowed to cool for a few minutes before measurements were taken. The solution of interest was placed in a sample vessel and left undisturbed in the tensiometer for 3–5 min. The sample vessel with the solution of interest was raised automatically by the tensiometer until it was in contact with the plate which was suspended perpendicular to the interface. All measurements were performed at 25 ± 1 °C. The tensiometer automatically detected the endpoint of each experiment and was set to terminate when the standard deviation between ten successive measurements were less than 0.01 or after 10 h had elapsed. Before each experiment the surface tension of water was measured to ensure accurate measurement and surface cleanliness. Repeatability was ensured as the standard deviations between the repeats for the four concentrations were within ± 0.3 mN m^{-1}. The standard deviation of the surface tension between 10 h and half an hour were found to be within ± 0.001 mN m^{-1}. Therefore the surface tensions for the remaining concentrations were measured for half an hour.

The CMC was determined via a plot of equilibrium surface tension against concentration. The maximum surface concentration and Langmuir constant were calculated using the surface equation of state for the Langmuir isotherm obtained by the Gibbs adsorption equation (Chang and Franses, 1995) as shown in Eq. (1).

$$\Pi = \gamma_0 - \gamma = nRT\Gamma_m \ \ln(1 + K_L c) \quad (1)$$

where Π is the surface pressure, γ_0 is the surface tension of the solvent, γ is the surface tension, R is the gas constant, T is temperature in Kelvin, c is the bulk concentration, Γ_m is the maximum surface concentration and K_L is the Langmuir constant and n is a constant which depends on the surfactant. For an ionic surfactant $n=2$ and for a nonionic surfactant $n=1$.

Γ_m and K_L were determined by fitting Eq. (1) to experimental equilibrium surface tension data using the solver tool in Microsoft Excel.

2.3.2. Nuclear magnetic resonance (NMR)

1D ^{1}H NMR experiments were performed on a 600 MHz Bruker Avance spectrometer using a TXI cryoprobe equipped with z gradients and 0.5 ml of sample solutions in 5 mm thin walled tubes. 1D ^{1}H NMR spectra were acquired from a standard pulse programme from Bruker Topsin software called stebpgp1s19. This pulse sequence consisted of stimulated echo, unbalanced bipolar gradient, spoil gradients and a 3-9-19 pulse train. The temperature was kept constant at 298 K.

Data was acquired for gradient strength ranging from 0.681 G cm^{-1} to 32.4 G cm^{-1} for BSA using a gradient pulse time (∂) of 6×10^{-3} s, diffusion time (Δ) of 0.15 s and correction time for bipolar gradient (τ_n) of 2.17×10^{-4} s. For Triton X−100 the gradient strength was varied from 0.681 G cm^{-1} to 33.4 G cm^{-1} using a ∂ of 1×10^{-3} s, Δ of 0.5 s and τ_n of 2.17×10^{-4} s. The relaxation delay time between repeated scans was equal to 2.5 s. The number of scans performed for BSA and Triton X−100 varied from 32 to 64 depending on the concentration of the sample. NMR spectra was obtained for Triton X−100 for concentrations of 1×10^{-5}, 3×10^{-5},1×10^{-4} and 1×10^{-3} mol L^{-1} and BSA for concentrations of 1×10^{-5}, 5×10^{-5} and 1×10^{-4} mol L^{-1}.

The diffusion coefficient was calculated by fitting Eq. (2) (Claridge, 2009) to a plot of experimental intensity against gradient strength

$$I = I_o e^{-D\gamma_n^2 G^2 \partial^2 (\Delta - \partial/3 - \tau/2)} \quad (2)$$

where I is the observed instensity, I_o is the reference unattenuated signal intensity, D is the diffusion coefficient γ_n is the magnetogyric ratio which is a property of the nuclei (for ^{1}H, γ_n = 26751 rad s^{-1} G^{-1}), G is the gradient strength, ∂ is the gradient pulse time, Δ is diffusion time and τ is a correction time for the time between the bipolar gradient.

2.3.3. Bubble size measurement

The foam bubble size was measured by performing batch and continuous foam fractionation experiments and then collecting the foam produced in a glass container of square cross section with a glass prism attached to one face of the container. This set up allowed two dimensional images of the bubble cross section against the glass container wall to be obtained by taking photos through one face of the prism parallel to the lens of the camera.

Batch foam fractionation experiments were performed at an air flow rate of 1.2 L min^{-1} for aqueous solutions of pure Triton X – 100, pure BSA and their mixtures. Continuous foam fractionation was performed for Triton X – 100 and BSA mixture at an air flow rate of 1.2 L min^{-1}. The concentration of pure Triton X – 100 and pure BSA used were 7.73×10^{-5} mol L^{-1} and 3.03×10^{-5} mol L^{-1} respectively (The CMCs of Triton X – 100 and BSA are determined in Section 3.1). A significantly higher concentration of BSA than its CMC was required to form stable foam. For the mixtures, the concentration of Triton X – 100 and BSA were 3.09×10^{-4} mol L^{-1} and 3.03×10^{-6} mol L^{-1} respectively.

A Canon EOS 7D camera with macro lens was used to take the photos. The images were then analysed using ImageJ, an open source image processing and analysis package. A circular sticker of diameter 19 mm was placed on the container on the same plane as the foam. The images were calibrated by calculating the number of pixels per unit area for the known area of the circular sticker. The bubbles were assumed to be spherical hence the bubble diameter could be calculated. Previous studies, most notably Cheng and Lemlich (1983), have described in detail the errors associated with measuring foam bubble size distributions via imaging of bubbles against a glass surface and the methodology to infer 3-D size distributions from 2-D images. In conclusion, they found that the errors tended to cancel each other out."

To prevent sampling bias five images were analysed for each air flow rate for the batch experiments. Five images were also analysed for each time interval for the continuous foam fractionation experiment. Between 600 and 4000 bubbles were analysed for each image depending on the component. Care was taken when analysing bubble size by disregarding incorrectly analysed bubbles; for instance when several bubbles were measured as a single bubble. The bubble sizes from the five images were then combined to obtain smooth distribution of bubble sizes. The representative bubble diameter for each air flow rate was the Sauter mean diameter, d_{32}, of the five images.

2.3.4. Foam fractionation experiment

Triton X – 100 and BSA mixtures were separated using a continuous foam fractionation system in stripping mode shown in Fig. 1. 12 l of Triton X – 100 and BSA mixtures were fed into the top of the straight section of a "J" shaped glass column of diameter, d, 50 mm and height, H, 440 mm via a peristaltic pump and a metal tube distributor at a feed flow rate of 30 ml min^{-1}. Humidified air was sparged through a sintered glass disk into a liquid pool creating overflowing foam. The initial composition of the liquid pool at the bottom of the column was the same as the feed and exited the column through an exit port in such a way that a constant liquid level of 100 ± 10 mm was maintained throughout the experiment. The enriched overflowing foam was collected at the open end of the "J" shaped section. The liquid pool and foam that exited the foam fractionation column is referred to as the retentate and foamate respectively throughout this paper.

Experiments were performed for four different feed concentrations of Triton X – 100 and BSA and five different air flow rates of 0.5, 0.9, 1.2, 2 and 3 L min^{-1} as shown in Table 1. All the other parameters such as feed flow rate and liquid pool level were the same for all experiments. Foam fractionation was performed for 6 h to ensure steady state conditions and feed, retentate and foamate samples were collected every hour. The foamate samples were made air tight to prevent evaporation and placed in the fridge maintained at a temperature of 4 °C overnight to collapse. The foamate samples were then diluted ten times with bi distilled water. The feed, retentate and diluted foamate samples were analysed using reverse phase HPLC.

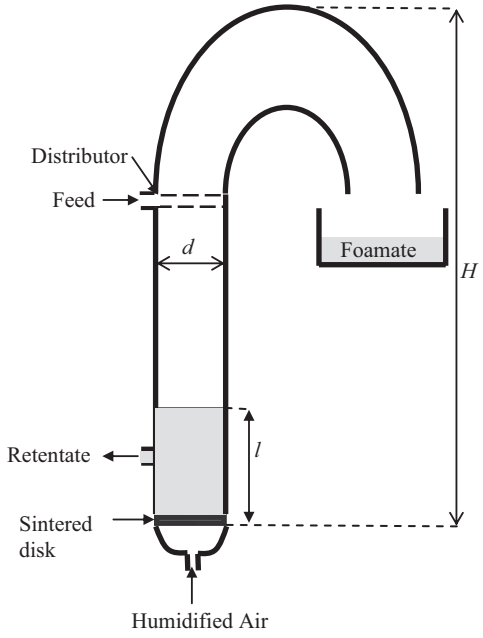

Fig. 1. Schematic diagram of foam fractionation experimental set up.

Table 1
Foam fractionation experiments.

Experiment	Feed concentration (mol L^{-1})		Air flow rate (L min^{-1})
	BSA	Triton X – 100	
1	3.03×10^{-6}	3.09×10^{-4}	0.5, 0.9, 1.2, 2 and 3
2	1.52×10^{-6}	1.55×10^{-4}	0.5, 0.9, 1.2, 2 and 3
3	3.03×10^{-6}	1.55×10^{-4}	0.5, 0.9, 1.2, 2 and 3
4	3.03×10^{-6}	3.86×10^{-5}	0.5, 0.9, 1.2, 2 and 3

The quantity of retentate and foamate exiting the column were continuously recorded throughout the experiment using digital balances (Ohaus,CH) connected to a custom data logging software from which the mass flow rates of the retentate and foamate were determined. The mass of the feed was weighed before and after the experiment from which the mass flow rate of the feed was calculated. The mass balance for most foam fractionation experiments balanced to within 5%.

The separation performance of a foam fractionation process is generally characterised by two parameters; the enrichment and recovery. Enrichment is the ratio of the concentration of the desired surface active molecule in the foamate to that in the feed solution (Eq. (3)) and recovery is the percentage of the desired molecules initially in the feed that is recovered in the foamate product (Eq. (4)).

$$Enrichment = \frac{c_F}{c_{in}} \tag{3}$$

$$Recovery = \frac{c_F Q_F}{c_{in} Q_{in}} \times 100 \tag{4}$$

where c_F is the concentration of surfactant concentration in the foamate, c_{in} is the concentration of surfactant in the feed, Q_F is the volumetric flowrate of foamate and Q_{in} is the volumetric flowrate of the feed

2.3.5. High performance liquid chromatography (HPLC) method

HPLC is a chromatographic separation method that is typically operated with blends of solvents (mobile phase A and B), where the relative amounts of these phases determines the rate at which material is eluted out of the column. The separation of mixed surfactant protein systems by HPLC reported in literature is relatively uncommon. In most of these studies surfactants such as Triton X–100 were added to proteins such as plasma proteins and vaccines for virus inactivation or to prevent protein aggregation during the manufacturing process. HPLC is then used to separate the added surfactants from the protein biomolecule (Heinig and Vogt, 1997; Karlsson et al., 2002; Gorka et al., 2012).

In literature different gradient and isocratic methods have been reported for BSA (Ferreira et al., 2001; Fernández et al., 2011) and Triton X – 100 (Heinig and Vogt, 1997; Vanhoenacker and Sandra, 2005). Ferreira et al. (2001) used a gradient elution method with the same mobile phase solvents used in this study for the HPLC analysis of bovine milk proteins. A linear gradient of 37–47% of mobile phase B was set for 5 min. This gradient was maintained for 2 min and was followed by another linear gradient of 47–52% for 5 min. After which the gradient was set back to 36% for 2 min. Heinig and Vogt (1997) reported on an isocratic mode of mobile phase acetonitrile/water (70:30) ratio for the separation of Triton X – 100 from influenza vaccine. Vanhoenacker and Sandra (2005) reported on an isocratic mode of mobile phase acetonitrile/water (50:50) ratio for the determination of Triton X – 100.

A new method for the separation of Triton X–100/BSA mixture based on blend of aforementioned published methods along with optimisation of mobile phase is reported in this paper. The concentration of Triton X–100 and BSA were determined by reverse phase HPLC using a Dionex Ultimate 3000 HPLC system. A Thermofisher acclaim 120 column of dimensions 150 mm × 4.6 mm, a particle size of 5 μm and a pore size of 120 Å was used. Table 2 shows the gradient elution method used for identification of Triton X–100 and BSA. The mobile phase consisted of 0.1% (v/v) triflouroacetic acid (TFA) in water (mobile phase A) and 0.1% (v/v) TFA in acetonitrile (ACN) (mobile phase B) was set at a flow rate of 1 ml min^{-1}. The column was placed in an oven maintained at a temperature of 40 °C. 20 μl of the samples was injected into the column and the output was detected by a UV spectrometer at wavelength of 220 nm.

Six standards of concentrations were used for each component for HPLC analysis and the calibration plots for both components are shown in Fig. 2. The R^2 values for Triton X – 100 and BSA were 0.9993 and 0.9996 respectively. For each HPLC analysis, pure Triton X – 100 and BSA calibration standards were run alongside the

Table 2
Gradient elution method for HPLC separation of Triton X – 100 and BSA mixture.

Time (min)	% mobile phase B
0	25
4	48
10	48
12	55
35	55
37	25
45	25

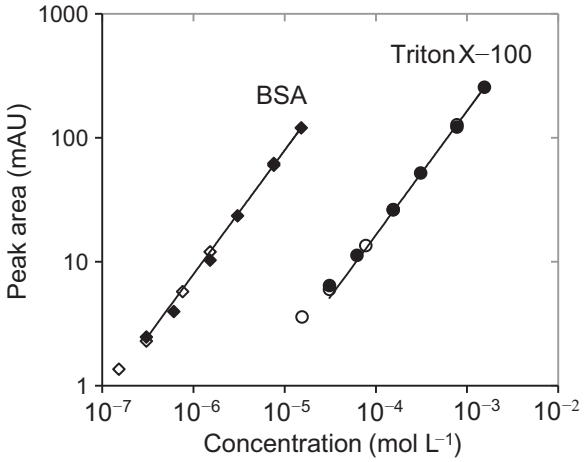

Fig. 2. HPLC calibration data for Triton X – 100 and BSA. Pure BSA (♦), pure Triton X – 100 (•), BSA in mixture (◇), Triton X – 100 in mixture (○) The black lines are linear trend lines for the standards of pure Triton X – 100 and BSA.

foam fractionation samples and calibration was accepted if the plot of peak area against concentration gave a R^2 value equal or greater than 0.999. To ensure there was no interaction between Triton X – 100 and BSA resulting in loss of material in the HPLC column, Triton X – 100/BSA mixtures of known concentrations were analysed and the calibration plots for the mixed samples are also shown in Fig. 2.

Except for the lowest concentrations, the percentage errors between the measured and known concentrations for Triton X – 100 and BSA in the mixed samples were less than 5%. For the lowest concentrations of Triton X – 100 and BSA the percentage error were 40% and 13%, respectively. This meant low accuracy of concentration measurements for concentrations below 1.55×10^{-5} mol L^{-1} and 1.52×10^{-7} mol L^{-1} for Triton X – 100 and BSA respectively, however these concentrations for Triton X – 100 and BSA are an order of magnitude lower than the feed concentrations of Triton X – 100 and BSA used in the foam fractionation experiments, given in Table 1.

3. Results and discussion

This study investigates the competitive adsorption behaviour of surfactants and proteins in a foam fractionation column. The results in this study are presented in the following order. Section 3.1 presents the surface tension profiles for aqueous solutions of pure Triton X – 100, pure BSA and Triton X – 100/BSA mixtures.. In Section 3.2 the diffusion coefficient of Triton X – 100 and BSA calculated from experimental NMR data is presented. The bubble size of foamate produced from batch and continuous foam fractionation experiments are presented in Section 3.3. In Section 3.4 the foam fractionation results are presented. Section 3.5 discusses and summarises the results presented in this paper.

3.1. Surface activity

The surface tension against concentration curves for all the components are shown on Fig. 3. The equilibrium surface tension for all components dropped with increasing concentration until the critical micelle concentration (CMC) was reached. Clear discontinuities in the plots defining the CMCs were observed for both components. The CMCs for Triton X – 100 and BSA were found be 2.5×10^{-4} mol L^{-1} and 1.4×10^{-7} mol L^{-1} respectively, in agreement with values reported by Wu et al. (1999) and Hossain and Fenton (1998) respectively. Two sets of surface tension against concentrations data was obtained for Triton X – 100 /BSA mixture.

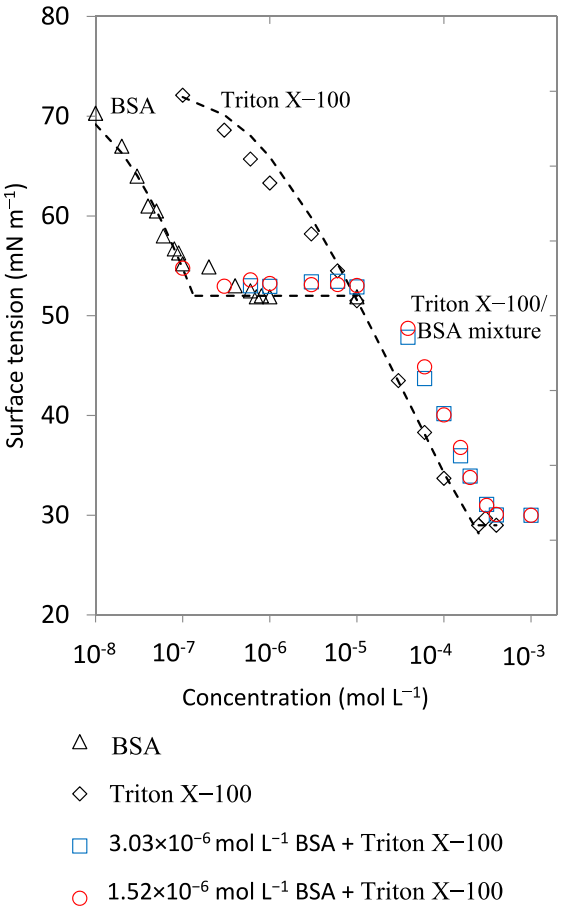

Fig. 3. Equilibrium surface tension against concentration plot for Triton X – 100 and BSA. Dashed lines show fitted Gibbs adsorption equation. For the mixtures, the concentration of BSA was kept constant whilst the concentration of Triton X – 100 was varied as shown by the x axis.

One with constant concentration of BSA at 3.03×10^{-6} mol L^{-1} and varying concentration of Triton X – 100 and the other with constant concentration of BSA at 1.52×10^{-6} mol L^{-1} and varying concentration of Triton X – 100. The concentrations of BSA and Triton X – 100 for the mixtures were selected to match the feed concentrations of BSA and Triton X – 100 used in the foam fractionation experiments given in Table 1. The surface tension against Triton X – 100 concentration profiles for Triton X – 100 /BSA mixtures were found to plateau when the concentration of Triton X – 100 in the mixture was 4×10^{-4} mol L^{-1}.

The surface tension remained constant for the mixtures until the concentration of Triton X – 100 in the mixture was 1×10^{-5} mol L^{-1}, where the surface tension of the mixture was similar to the surface tension of pure BSA at concentrations 3.03×10^{-6} mol L^{-1} and 1.52×10^{-6} mol L^{-1} at 53 mN m^{-1}. After which the surface tension of the mixture dropped sharply to 30 mN m^{-1}, similar to the surface tension of pure Triton X – 100.

The parameters Γ_m and K_L were determined using Eq. (1) for concentrations below the CMC as the Gibbs adsorption equation only applies to concentrations below the CMC. The Γ_m and K_L values for Triton X – 100 were determined to be 3.17×10^{-6} mol m^{-2} and 1500 m^3 mol^{-1} respectively and were in agreement with values reported by Mitrancheva et al. (1996) and Chang and Franses (1995) respectively. The Gibbs isotherm assumes reversible adsorption and hence is not applicable for BSA (Graham and Phillips, 1979; Douillard et al., 1993).

3.2. Diffusion coefficient

The diffusion coefficient was determined by finding the best fit of Eq. (2) to experimental NMR intensity against gradient strength for three prominent peaks in the spectra for different concentrations for both components. Eq. (2) fitted well to each individual peak for all samples. The diffusion coefficient for each concentration was calculated by taking the mean of the diffusion coefficients for each of the three peaks. This was repeated for each concentration and both components.

For Triton X – 100, the diffusion coefficient fitted for the three peaks for each concentration was relatively constant with standard deviations calculated to be less than 9.11×10^{-11} m^2 s^{-1}. The mean diffusion coefficient calculated for the highest concentration of 1×10^{-3} mol L^{-1} was lower than the diffusion coefficient calculated for the other concentrations. This could be because the highest concentration is about an order of magnitude greater than the CMC. Therefore micelle formation and self-aggregation affects the monomer diffusion coefficient calculated for Triton X – 100 (Cui et al., 2008). For BSA, the diffusion coefficient fitted for the three peaks for each concentration was relatively constant with standard deviations calculated to be less than 9.33×10^{-12} m^2 s^{-1}. The mean diffusion coefficient for the lowest concentration of 1×10^{-5} mol L^{-1} for all three peaks was 1.33 times greater than the diffusion coefficient for the other two concentrations.

Fig. 4 presents the mean diffusion coefficient against concentration for Triton X – 100 and BSA. Error bars are not shown since the standard deviation of the diffusion coefficients fitted to the three peaks was smaller than the symbols. The overall mean diffusion coefficient for Triton X – 100 for concentrations below the CMC was calculated to be 1.2×10^{-9} m^2 s^{-1}. The overall mean diffusion coefficient for BSA was calculated to be 6.11×10^{-11} m^2 s^{-1}. The results show that the diffusion coefficient of Triton X – 100 was two orders of magnitude greater than BSA.

3.3. Bubble size

The bubble size of foamate produced from batch foam fractionation of solutions of Triton X – 100, BSA and their mixtures an air flow rate of 1.2 L min^{-1} was measured. Fig. 5 presents the bubble size distributions of Triton X – 100, BSA and their mixtures. The bubble size distribution of BSA was found to have greater bubble sizes than Triton X – 100 where d_{32} of BSA was calculated to be 1.99 mm whilst d_{32} of Triton X – 100 was calculated to be 1.11 mm.

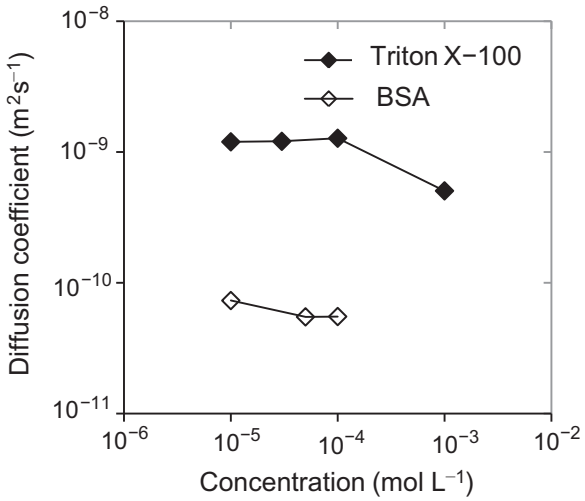

Fig. 4. Diffusion coefficient of Triton X – 100 and BSA.

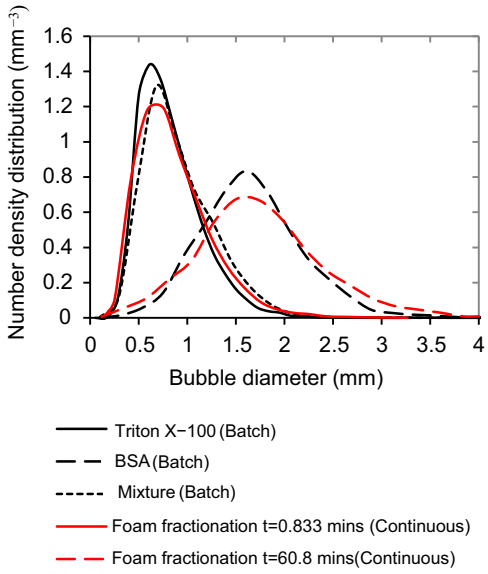

Fig. 5. Bubble size-continuous and batch foam fractionation experiments.

It was hypothesised that the bubble size distribution for Triton X−100/ BSA mixtures would be somewhere in between the bubble size distributions obtained for the two components. However as seen in Fig. 5 the bubble size distributions of the mixtures obtained had similar trends to that of Triton X−100 with d_{32} of Triton X−100/ BSA mixtures calculated to be 1.22 mm. The concentration of pure Triton X−100 was 7.73×10^{-5} mol L^{-1} whilst the concentration of Triton X−100 in the mixture was 3.09×10^{-4} mol L^{-1}. Hence the similar bubble size trends of pure Triton X−100 and Triton X−100/BSA mixtures indicate that the bubble size was not significantly affected by concentration range of Triton X−100 used for the bubble size measurements.

Next the bubble size of the foamate produced during continuous foam fractionation of Triton X−100/BSA mixtures was measured at an air flow rate of 1.2 L min^{-1}. The feed and initial liquid pool concentrations for both Triton X−100 and BSA were 3.09×10^{-4} mol L^{-1} and 3.03×10^{-6} mol L^{-1} respectively (The CMCs of Triton X−100 and BSA are determined in Section 3.1 to be 2.5×10^{-4} mol L^{-1} and 1.4×10^{-7} mol L^{-1} respectively). The bubble size of the foamate was measured at t=0.833 min (50 s) when the foam first left the column and t=60.8 min (1 h after the initial foam was produced and at steady state conditions).

Fig. 5 presents the bubble size distributions of the foamate produced from continuous foam fractionation of Triton X−100/ BSA mixtures. Initially at t=0.833 min the bubble size distribution from the continuous foam fractionation resembles that of pure Triton X−100 and Triton X−100/BSA mixtures from the batch foam fractionation experiments. After 1 h of foam fractionation the bubble size distribution is observed to shift towards the bubble size distribution of pure BSA. The foam collected at t=0.833 min would have been formed from the initial liquid pool which had the same composition as the mixtures used in the batch experiments. This was confirmed through the similar trend of the bubble size distribution for the continuous foam fractionation at t=0.833 min and the bubble size distribution of the mixtures from the batch foam fractionation experiments. The shifting of the bubble size distribution after one hour to the bubble distribution of pure BSA suggests that over time the liquid pool mostly consists of BSA and the air bubbles rising from the liquid pool are mostly stabilised by adsorbed BSA.

In addition, the measured pool concentration of Triton X−100 (from HPLC measurements of retentate samples at one hour intervals throughout the foam fractionation process) was found to be too low to produce stable foam. The measured retentate concentrations are indicative of the bottom liquid pool concentrations. The measured retentate concentrations of Triton X−100 and BSA were 1.60×10^{-8} mol L^{-1} and 2.53×10^{-6} mol L^{-1} respectively.

The foamability of Triton X−100 at low concentrations was tested by sparging air into a liquid pool of different concentrations of Triton X−100 in the foam fractionation column. For the lowest concentration of 1.55×10^{-6} mol L^{-1} no significant amount of foam was produced and this concentration was two orders of magnitude higher than the measured retentate concentration of Triton X−100 of 1.60×10^{-8} mol L^{-1}.

Similar to Triton X−100, the bubble size of BSA was shown to be unaffected by concentrations used, where the bubble size distributions of pure BSA from the batch foam fractionation experiments and the continuous foam fractionation at t=60.8 min are shown to resemble each other. The concentration of pure BSA was 3.03×10^{-5} mol L^{-1} whilst the concentration of BSA in the liquid pool at t=60.8 min was measured to be 2.58×10^{-6} mol L^{-1}.

The above results suggest that the bubble size was not significantly affected by the concentration range of Triton X−100 and BSA used for the bubble size measurements but by the type of surface active molecule.

3.4. Foam fractionation

Foam fractionation separation performance was evaluated in terms of recovery and enrichment. Fig. 6 shows the recovery and enrichment variation with increasing air flow rate for all experiments. The repeatability of the foam fractionation experiments was tested for experiment 1 with an air flow rate of 1.2 L min^{-1} and the standard deviation for the recovery and enrichment of Triton X−100 and BSA for two runs were calculated to be $\pm$0.03% and $\pm$0.2 respectively (The error bars in Fig. 6(a) are the standard deviation for these two runs). Although some of the recovery values determined were above 100%, all the values were within the mass balance error of 5% calculated for all foam fractionation experiments, with the highest recovery value being 103%.

In experiment 1 and 2 the recovery and enrichment of Triton X−100 increased and decreased respectively with increasing air flow rate. This response is typical for a single component system where with increasing air flow rate the residence time of the bubbles in the column decreases resulting in less net drainage and wetter foams. Hence enrichment is reduced while recovery is enhanced. However, in contrast to Triton X−100 the recovery and enrichment of BSA both increased with increasing air flow rate. This observation indicates a different behaviour to that of a single component system. At low air flow rates for experiment 1 the recovery of Triton X−100 is below 100%. For these air flow rates the enrichment of BSA remained at one and only began to increase once the recovery of Triton X−100 reached 100%. In experiment 2 the recovery of Triton X−100 was already at 100% at the lowest air flow rate and the enrichment of BSA increased with increasing air flow rate. This behaviour suggests that BSA only adsorbed to the surface once all Triton X−100 had adsorbed demonstrating competitive adsorption behaviour.

The feed concentrations for both Triton X−100 and BSA in experiment 2 were half the feed concentrations in experiment 1. With a lower feed concentration of Triton X−100 and the same feed flow rate, it was expected that the air flow rate required to recover all of the Triton X−100 would decrease proportionately. The results appear to be in agreement with this hypothesis: the recovery at air flow rate of 0.5 L min^{-1} was 75% for a feed concentration of 3.09×10^{-4} mol L^{-1} in experiment 1 which

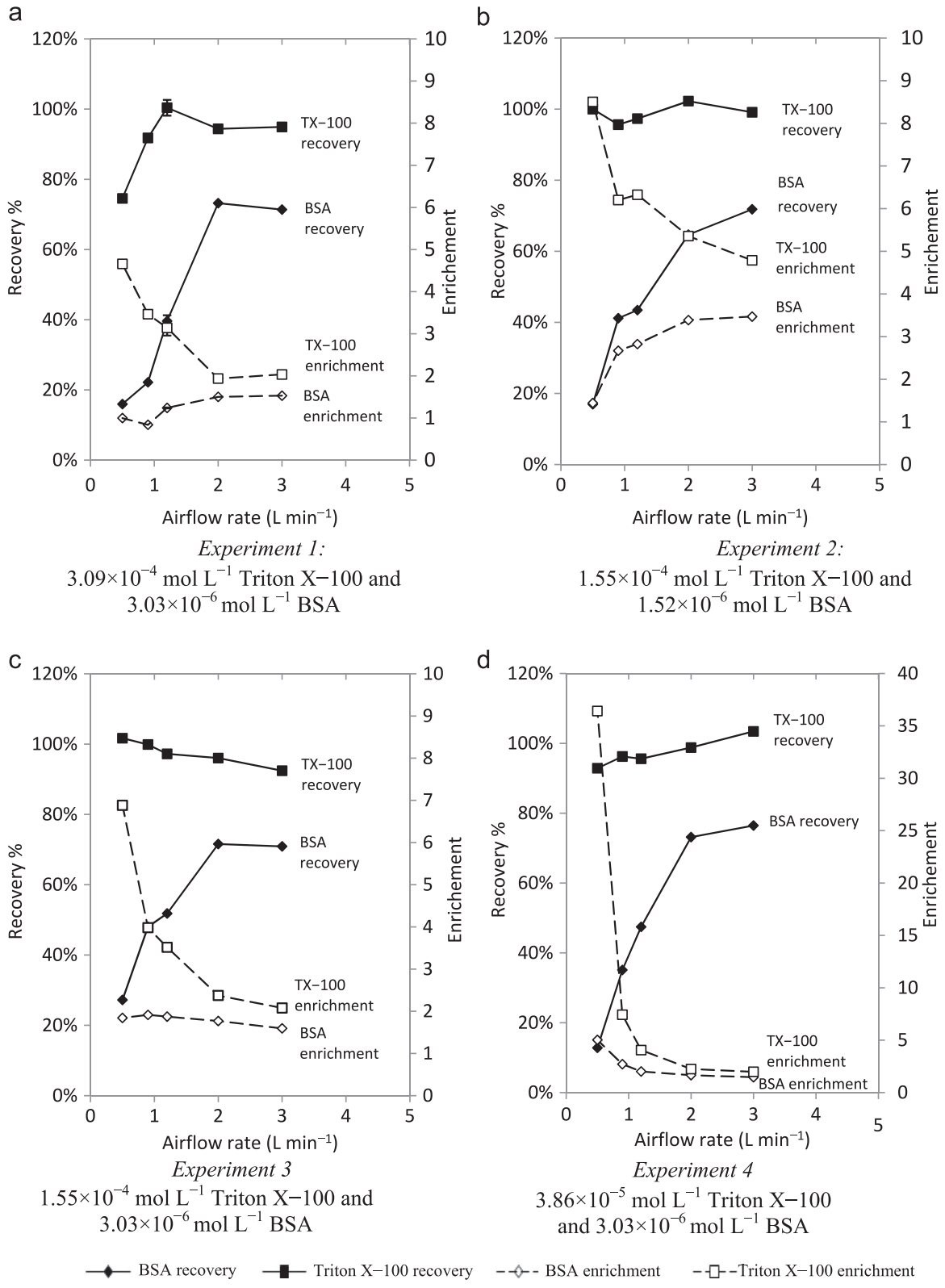

Fig. 6. Recovery and enrichment. Error bars in plot (a) are standard deviation of two experimental repeats of experiment 1 at an air flow rate of 1.2 L min^{-1} (a) *Experiment 1*:3.09×10^{-4} mol L^{-1} Triton X – 100 and 3.03×10^{-6} mol L^{-1} BSA (b) *Experiment 2:* 1.55×10^{-4} mol L^{-1} Triton X – 100 and 1.52×10^{-6} mol L^{-1} BSA (c) *Experiment 3* 1.55×10^{-4} mol L^{-1} Triton X – 100 and 3.03×10^{-6} mol L^{-1} BSA (d) *Experiment 4* 3.86×10^{-5} mol L^{-1} Triton X – 100 and 3.03×10^{-6} mol L^{-1} BSA.

increased to 100% for a feed concentration of 1.55×10^{-4} mol L^{-1} in experiment 2. Decrease in feed concentration was also expected to increase enrichment and this effect is observed via the shift upwards to greater enrichment values for both Triton X – 100 and BSA from experiment 1 to 2. The enrichment range for Triton X – 100 in experiment 1 was from 2 to 5 which increased to 5–8.5 in experiment 2. The enrichment range for BSA was 1–1.5 in experiment 1 which increased to 1.5 to 3.5 in experiment 2.

In the next set of experiments the objective was to explore conditions that would result in BSA behaving as a single component system. Hence in experiment 3 and 4 the feed concentration of BSA was kept constant at 3.03×10^{-6} mol L^{-1} whilst the feed concentration of Triton X−100 were lowered to 1.55×10^{-4} mol L^{-1} and 3.86×10^{-5} mol L^{-1}. Fig. 6(c) and (d) shows the recovery and enrichment of experiment 3 and 4 respectively with increasing air flow rate. The recovery and enrichment trends of BSA were found to behave more like that of a single component system.

The feed concentration of Triton X−100 in the mixture had a significant effect on the enrichment of both Triton X−100 and BSA in the foamate. The enrichments for Triton X−100 increased with decreasing Triton X−100 feed concentrations most notable at lower air flow rates. For example at an air flow rate of 0.5 L min^{-1} the enrichment of Triton X−100 increased from 4.66 to 36.4 when the feed concentration of Triton X−100 decreased from 3.09×10^{-4} mol L^{-1} (experiment 1) to 3.86×10^{-5} mol L^{-1} (experiment 4). The same effect was also observed for BSA where the enrichment of BSA increased with decreasing Triton X−100 feed concentration. The enrichment drop of BSA and Triton X−100 with increasing air flow rate was more pronounced with decreasing feed concentration of Triton X−100. For example the enrichment of BSA dropped by 0.320 for a Triton X−100 feed concentration of 1.55×10^{-4} mol L^{-1} (experiment 3) and 3.55 for a Triton X−100 feed concentration of 3.86×10^{-5} mol L^{-1} (experiment 4).

In experiment 1 and 2 the different recovery and enrichment behaviour of BSA with increasing air flow rate could be because of the different adsorption and diffusion properties of Triton X−100 and BSA summarised in Table 3. The surface activity and diffusion parameters shown in Table 3 were determined and calculated in Sections 3.1 and 3.2. From Table 3 it is seen that Triton X−100 is a smaller molecule with higher surface pressure, higher diffusion coefficient and higher surface activity than BSA. This means that Triton X−100 diffuses to the surface and adsorbs at the surface faster and to a greater extent than BSA. Hence in the presence of Triton X−100 and BSA, surface adsorption will always be dominated by Triton X−100.

Thus in experiment 1, the enrichment of BSA remains at unity with increasing air flow rate until the recovery of Triton X−100 reached 100%. That is BSA only began to adsorb once all Triton X−100 molecules adsorbed. In experiment 2 the enrichment of BSA increased with increasing air flow rate as Triton X−100 had already reached 100% recovery at the lowest air flow rate.

In experiment 3 and 4 BSA was found to show trends similar to that of a single component system. This could be due to the lower feed concentrations of Triton X−100 compared to experiments 1 and 2, resulting in fewer Triton X−100 molecules competing with BSA at the surface.

Table 3
Surface activity and diffusion properties of Triton X−100 and BSA.

Properties	Triton X−100	BSA
Molecular weight (kDa)	0.63	66
CMC (mol m^{-3})	0.25	1.4×10^{-4}
Equilibrium surface tension at CMC, γ_{CMC} (mN m^{-1})	30	52
Surface pressure at CMC, Π (mN m^{-1})	43	21
Diffusion coefficient (m^2 s^{-1})	1.2×10^{-9}	6.11×10^{-11}

3.5. Discussion and summary

The recovery and enrichment results presented in this paper showed that 75–100% of Triton X−100 and 13–76% of BSA was recovered in the foamate in most of the foam fractionation experiments. Thus the recovery of BSA was always lower than Triton X−100. The bubble size distribution results demonstrated that the bubbles rising from the liquid pool at the beginning of the process were stabilised by Triton X−100, whereas after steady state conditions were established the bubbles rising from the liquid pool were stabilised by BSA.

These results suggest two possible scenarios. One is that Triton X−100 entering the column from the feed flow at the top of the column displaced BSA from the bubbles rising up the column. The second is that Triton X−100 from the feed co-adsorbed or formed a surface layer on top of the BSA stabilised bubbles rising up the column. If the second scenario occurred then it would be expected to yield a high enrichment of BSA in the foamate due to that adsorbed on the surface. However, BSA enrichment in the foamate was almost unity for all experiments with higher Triton X−100 feed concentrations at low air flow rates. Thus, it is concluded that the phenomena of the first scenario occurred, where Triton X−100 displaced the adsorbed BSA from the surface.

BSA has been reported to have irreversible adsorption at the air–water surface where Svitova et al. (2003) reported that BSA exhibited complete irreversibility after 4 h of contact with the air-water surface. In this case the initial BSA solution was replaced with wash out water. However a study more recently performed by Vaidya and Narváez (2014) showed that when the initial BSA solution was replaced by an aqueous solution of Triton X−100, the pre-adsorbed layer of BSA was displaced by Triton X−100 molecules at the air-water surface.

Likewise, the results from the experiments in this paper indicate displacement of BSA by Triton X−100. If BSA/ Triton X−100 complexes were formed they would be either in the bulk solution or adsorbed on the foam surface. If these complexes were in the bulk solution then some would drain with the liquid into the bottom pool and be found in the retentate. However negligible Triton X−100 was measured in the retentate stream, so this does not appear to be occurring. If these complexes were adsorbed onto the foam surface then some BSA enrichment in the foamate would be expected in all cases. The results on Fig. 6 show a range of conditions where almost no BSA enrichment in the foamate occurred, so it appears that complexes did not occur on the foam surfaces. Furthermore, several authors (Makino et al., 1973; Clarke, 1977; Ghosh and Dey, 2015) have reported that little complex formation occurs between Triton X−100 and BSA.

The competitive adsorption behaviour of Triton X−100 and BSA in the foam fractionation column was elucidated in terms of the differences in surface activity and diffusivity of Triton X−100 and BSA. The Triton X−100 maximum surface pressure is a factor of 2.05 that of BSA and the Triton X−100 diffusion coefficient of is a factor of 19.6 that of BSA. Therefore Triton X−100 is more surface active and has higher diffusivity than BSA. Triton X−100 dominates the surface adsorption by diffusing to the surface and adsorbing at the surface faster and to a greater extent than BSA. Thus for high feed concentrations of Triton X−100 (experiments 1 and 2) in the foam fractionation experiments, the recovery and enrichment of BSA was found to be low and show a different trend with increasing air flow rate than that of a single component system. However BSA was found to behave more like a single component system with increased enrichment once the feed concentration of Triton X−100 was an order of magnitude lower than its CMC (experiment 3 and 4). For example in experiment 4 at an air flow rate of 0.5 L min^{-1} the enrichment of BSA was about five times greater than that of experiment 1. This suggests

that at low feed concentration of Triton X – 100 there is more surface space available for BSA adsorption thereby exhibiting increased BSA enrichment. The surface adsorption domination of Triton X – 100 over BSA was also observed by the bubble size distribution results of Triton X – 100/BSA mixtures from the batch foam fractionation experiments where the bubble size distributions of foams formed from Triton X – 100/BSA mixtures resembled that of pure Triton X – 100 suggesting surface adsorption domination by Triton X – 100.

4. Conclusion

It was shown that the results presented in this paper could physically describe the competitive adsorption and transport process of Triton X – 100/BSA mixtures in the foam fractionation column. The bubble size results demonstrated that the bubbles rising from the liquid pool were stabilised by BSA however the recovery and enrichment foam fractionation results showed that the recovery and enrichment of Triton X – 100 was always greater than that of BSA. In addition for high feed concentrations of Triton X – 100, the enrichment of BSA remained at unity until the recovery of Triton X – 100 reached 100%. Thus it was concluded that Triton X – 100 entering the column from the feed flow at the top of the column displaced adsorbed BSA from the surface of the bubbles rising up the column.

This competitive adsorption behaviour was elucidated by the surface activity and transport properties of Triton X – 100 and BSA, determined from surface tension and NMR measurements. The maximum surface pressure and diffusivity of Triton X – 100 was found to be 2.05 and 19.6 times respectively greater than BSA. Therefore Triton X – 100 dominated the surface adsorption by diffusing to the surface and adsorbing at the surface faster and to a greater extent than BSA. This resulted in greater separation of Triton X – 100 compared to BSA.

The research in this paper takes a step beyond the literature experimental foam fractionation studies for multicomponent systems. Through careful measurement and experimental design this study has achieved a deeper understanding of the transport and competitive adsorption kinetics of two surface active components in a foam fractionation column This present study demonstrates how foam fractionation experiments can be supported with simple experiments such as surface tension, NMR and foam bubble size measurements to provide a deeper insight and knowledge of the competitive adsorption behaviour of compounds in a foam fractionation process.

Notation

c	Concentration (mol m^{-3})
d	Column diameter (m)
d_{32}	Sauter mean diameter (m)
D	Diffusion coefficient (m^2 s^{-1})
g	Gravitational acceleration (m s^{-2})
G	Gradient strength (G cm^{-1})
H	Column height (m)
I	Observed NMR instensity (dimensionless)
I_o	Reference unattenuated signal intensity (dimensionless)
K_L	Langmuir constant (m^3 mol^{-1})
n	Number of surfactant species (dimensionless)
Q_F	Volumetric flow rate (m^3 s^{-1})
R	Gas constant (m^3 Pa K^{-1} mol^{-1})
T	Temperature (K)

Greek symbols

γ	Surface tension (mN m^{-1})
γ_0	Surface tension of solvent (mN m^{-1})
γ_n	Magnetogyric ratio (rad s^{-1} G^{-1})
Γ_m	Maximum surface concentration (mol m^{-2})
τ	Bipolar gradient correction time (s)
∂	Gradient pulse time (s)
Δ	Diffusion time (s)
Π	Surface pressure (mN m^{-1})

Subscripts

0	Zero
F	Foamate
in	Feed
max	Maximum

Acknowledgements

The authors gratefully acknowledge the assistance of Dr Matt Cliff in obtaining the NMR results. The authors are grateful for financial support from the UK Engineering and Physical Sciences Research Council (EP/I024905) which enabled this work to be conducted.

References

Brown, A.K., Kaul, A., Varley, J., 1999. Continuous foaming for protein recovery: Part II. Selective recovery of proteins from binary mixtures. Biotechnol. Bioeng. 62, 291–300.
Burghoff, B., 2012. Foam fractionation applications. J. Biotechnol. 161, 126–137.
Chang, C.H., Franses, E.I., 1995. Adsorption dynamics of surfactants at the air/water interface: a critical review of mathematical models, data, and mechanisms. Colloids Surf. A: Physicochem. Eng. Asp. 100, 1–45.
Cheng, H.C., Lemlich, R., 1983. Errors in the measurement of bubble size distribution in foam. Ind. Eng. Chem. Fundam. 22, 105–109.
Claridge, T.D.W., 2009. Diffusion NMR spectroscopy. In: Claridge, T.D.W. (Ed.), High-Resolution NMR Techniques in Organic Chemistry (Tetrahedron Organic Chemistry Series), 27. Elsevier, Amsterdam, The Netherlands, pp. 281–304.
Clarke, S., 1977. The interaction of Triton X – 100 with soluble proteins: possivle implications for the transport of proteins across membranes. Bichemical Biophys. Res. Commun. 79 (1), 46–52.
Coward, T., Lee, J.G.M., Caldwell, G.S., 2014. Harvesting microalgae by CTAB-aided foam flotation increases lipid recovery and improves fatty acid methyl ester characteristics. Biomass-. Bioenergy 67, 354–362.
Cui, X., Mao, S., Liu, M., Yuan, H., Du, Y., 2008. Mechanism of surfactant micelle formation. Langmuir 24, 10771–10775.
Douillard, R., Lefebvre, J., Tran, V., 1993. Applicability of Gibbs' law to protein adsorption isotherms. Colloids Surf. A: Physicochem. Eng. Asp. 78, 109–113.
Fernández, A., Menéndez, V., Riera, F.A., Álvarez, R., 2011. Caseinomacropeptide behaviour in a whey protein fractionation process based on α-lactalbumin precipitation. J. Dairy Res. 78, 196–202.
Ferreira, I.M., Mendes, E., Ferreira, M.A., 2001. HPLC/UV analysis of proteins in dairy products using a hydrophobic interaction chromatographic column. Anal. Sci. 17, 499–501.
Gerken, B.M., Nicolai, A., Linke, D., Zorn, H., Berger, R.G., Parlar, H., 2006. Effective enrichment and recovery of laccase C using continuous foam fractionation. Sep. Purif. Technol. 49, 291–294.
Ghosh, S., Dey, J., 2015. Interaction of bovine serum albumin with Nacyl amino acid based anionic surfactants: effect of head-group hydrophobicity. J. Colloid Interface Sci. 458, 284–292.
Gorka, J., Rohmer, M., Bornemann, S., Papasotiriou, D.G., Baeumlisberger, D., Arrey, T.N., Bahr, U., Karas, M., 2012. Perfusion reversed-phase high-performance liquid chromatography for protein separation from detergent-containing solutions: an alternative to gel-based approaches. Anal. Biochem. 424, 97–107.
Graham, D.E., Phillips, M.C., 1979. Proteins at liquid interfaces: II. Adsorption isotherms. J. Colloid Interface Sci. 70, 415–426.
Grassia, P., Ubal, S., Giavedoni, M.D., Vitasari, D., Martin, P.J., 2016. Surfactant flow between a plateau border and a film during foam fractionation. Chem. Eng. Sci. 143, 139–165.
Heinig, K., Vogt, C., 1997. Determination of Triton X-100 in influenza vaccine by high-performance liquid chromatography and capillary electrophoresis. Fresenius' J. Anal. Chem. 359, 202–206.

Hossain, M.M., Fenton, G., 1998. Application of foam separation processes for protein extraction/stripping. Australas. Biotechnol. 8, 289–294.
Karlsson, G., Hinz, A.C., Henriksson, E., Winge, S., 2002. Determination of Triton X−100 in plasma-derived coagulation factor VIII and factor IX products by reversed-phase high-performance liquid chromatography. J. Chromatogr. A 946, 163–168.
Lemlich, R., 1968. Adsorptive bubble separation methods—foam fractionation and allied techniques. Ind. Eng. Chem. 60, 16–29.
Lemlich, R., 1972. Adsorptive Bubble Separation Techniques. Academic Press, London.
Linke, D., Berger, R.G., 2011. Foaming of proteins: new prospects for enzyme purification processes. J. Biotechnol. 152 (4), 125–131.
Liu, W., Wu, Z., Wang, Y., Li, R., Ding, L., Huang, D., 2015. Rhamnolipid assisted recovery of lycopene from the tomato-based processing wastewater using foam fractionation. J. Food Eng. 164, 63–69.
Lockwood, C., Bummer, P., Jay, M., 1997. Purification of proteins using foam fractionation. Pharm. Res. 14, 1511–1515.
Lockwood, C.E., Jay, M., Bummer, P.M., 2000. Foam fractionation of binary mixtures of lysozyme and albumin. J. Pharm. Sci. 89, 693–704.
Lu, K., Zhang, X.L., Zhao, Y.L., Wu, Z.L., 2010. Removal of color from textile dyeing wastewater by foam separation. J. Hazard. Mater. 182, 928–932.
Mackie, A.R., 2004. Structure of adsorbed layers of mixtures of proteins and surfactants. Curr. Opin. Colloid Interface Sci. 9, 357–361.
Makievski, A.V., Fainerman, V.B., Bree, M., Wüstneck, R., Krägel, J., Miller, R., 1998. Adsorption of proteins at the liquid/air interface. J. Phys. Chem. B 102, 417–425.
Makino, S., Reynolds, J.A., Tanford, C., 1973. The binding of deoxycholate and Triton X-100 to proteins. J. Biol. Chem. 248, 4926–4932.
Martin, P.J., Dutton, H.M., Winterburn, J.B., Baker, S., Russell, A.B., 2010. Foam fractionation with reflux. Chem. Eng. Sci. 65, 3825–3835.
Micheau, C., Schneider, A., Girard, L., Bauduin, P., 2015. Evaluation of ion separation coefficients by foam flotation using a carboxylate surfactant. Colloids Surf. A: Physicochem. Eng. Asp. 470, 52–59.
Miller, R., Fainerman, V.B., Makievski, A.V., Krägel, J., Wüstneck, R., 2000. Adsorption characteristics of mixed monolayers of a globular protein and a non-ionic surfactant. Colloids Surfaces A: Physicochem. Eng. Asp. 161, 151–157.
Miller, R., Grigoriev, D.O., Aksenenko, E.V., Zholob, S.A., Leser, M.E., Michel, M., Fainerman, V.B., 2005. Thermodynamic and adsorption kinetic studies of protein+surfactant mixtures. In: Dickinson, E. (Ed.), . Food Colloids: Interactions, Microstructure and Processing. The Royal Society of Chemistry, Cambridge, Location, pp. 120–130.
Mitrancheva, J.V., Dushkin, C.D., Joos, P., 1996. Kinetics of the surface tension of micellar solutions: comparison of different experimental techniques. Colloid Polym. Sci. 274, 356–367.
Niño, M., Patino, J.M.R., 1998. Surface tension of bovine serum albumin and tween 20 at the air-aqueous interface. J. Am. Oil Chem.' Soc. 75, 1241–1248.
Qu, Y.H., Zeng, G.M., Huang, J.H., Xu, K., Fang, Y.Y., Li, X., Liu, H.L., 2008. Recovery of surfactant SDS and Cd^{2+} from permeate in MEUF using a continuous foam fractionator. J. Hazard. Mater. 155, 32–38.
Rujirawanich, V., Triroj, M., Pornsunthorntawee, O., Chavadej, J., Chavadej, S., 2012. Recovery of surfactant from an aqueous solution using continuous multistage foam fractionation: mixed surfactant system. Sep. Sci. Technol. 48, 757–765.
Saleh, Z.S., Hossain, M.M., 2001. A study of the separation of proteins from multicomponent mixtures by a semi-batch foaming process. Chem. Eng. Process.: Process. Intensif. 40, 371–378.
Stevenson, P., 2012. Foam Engineering: Fundamentals and Applications. John Wiley & Sons, Chichester, UK.
Svitova, T.F., Wetherbee, M.J., Radke, C.J., 2003. Dynamics of surfactant sorption at the air/water interface: continuous-flow tensiometry. J. Colloid Interface Sci. 261, 170–179.
Vaidya, S.V., Narváez, A.R., 2014. Understanding interactions between immunoassay excipient proteins and surfactants at air–aqueous interface. Colloids Surf. B: Biointerfaces 113 (0), 285–294.
Vanhoenacker, G., Sandra, P., 2005. High temperature liquid chromatography and liquid chromatography–mass spectroscopy analysis of octylphenol ethoxylates on different stationary phases. J. Chromatogr. A 1082, 193–202.
Vitasari, D., Grassia, P., Martin, P., 2013a. Simulation of dynamics of adsorption of mixed protein–surfactant on a bubble surface. Colloids Surf. A: Physicochem. Eng. Asp. 438, 63–76.
Vitasari, D., Grassia, P., Martin, P., 2013b. Surfactant transport onto a foam lamella. Chem. Eng. Sci. 102, 405–423.
Vitasari, D., Grassia, P., Martin, P., 2016. Surfactant transport onto a foam film in the presence of surface viscous stress. Appl. Math. Model. 40 (3), 1941–1958.
Walkowiak, W., Grieves, R.B., 1976. Foam fractionation of cyanide complex anions of Zn(II), Cd(II), Hg(II) and Au(III). J. Inorg. Nucl. Chem. 38, 1351–1356.
Winterburn, J.B., Martin, P.J., 2012. Foam mitigation and exploitation in biosurfactant production. Biotechnol. Lett. 34, 187–195.
Wu, N., Dai, J., Micale, F.J., 1999. Dynamic surface tension measurement with a dynamic wilhelmy plate technique. J. Colloid Interface Sci. 215, 258–269.
Xu, Z., Wu, Z., Zhao, Y., 2010. Foam fractionation of protein with the presence of antifoam agent. Sep. Sci. Technol. 45, 2481–2488.